GaInAsP/InP lateral-current-injection distributed feedback laser with a-Si surface grating

Takahiko Shindo,[1,*] Tadashi Okumura,[1] Hitomi Ito,[1]Takayuki Koguchi,[1] Daisuke Takahashi,[1] Yuki Atsumi,[1] Joonhyun Kang,[1] Ryo Osabe,[1] Tomohiro Amemiya,[1,2] Nobuhiko Nishiyama,[2] and Shigehisa Arai[1,2,]

[1]Department of Electrical and Electronic Engineering, Tokyo Institute of Technology, 2-12-1-S9-5 O-okayama, Meguro-ku, Tokyo 152-8552, Japan
[2]Quantum Nanoelectronics Research Center, Tokyo Institute of Technology, 2-12-1-S9-5 O-okayama, Meguro-ku, Tokyo 152-8552, Japan
**shindou.t.aa@m.titech.ac.jp*

Abstract: We fabricated a novel lateral-current-injection-type distributed feedback (DFB) laser with amorphous-Si (a-Si) surface grating as a step to realize membrane lasers. This laser consists of a thin GaInAsP core layer grown on a semi-insulating InP substrate and a 30-nm-thick a-Si surface layer for DFB grating. Under a room-temperature continuous-wave condition, a low threshold current of 7.0 mA and high efficiency of 43% from the front facet were obtained for a 2.0-μm stripe width and 300-μm cavity length. A small-signal modulation bandwidth of 4.8 GHz was obtained at a bias current of 30 mA.

OCIS codes: (140.5960) Semiconductor lasers.

References and links

1. P. Kapur, J. P. McVittie, and K. C. Saraswat, "Technology and reliability constrained future copper interconnects. I. Resistance modeling," IEEE Trans. Electron. Dev. **49**(4), 590–597 (2002).
2. P. Kapur, G. Chandra, J. P. McVittie, and K. C. Saraswat, "Technology and reliability constrained future copper interconnects. II. Performance implications," IEEE Trans. Electron. Dev. **49**(4), 598–604 (2002).
3. D. A. B. Miller, "Device requirements of optical interconnects to silicon chips," Proc. IEEE **97**, 1166–1185 (2009).
4. G. Chen, H. Chen, M. Haurylau, N. A. Nelson, D. H. Albonesi, P. M. Fauchet, and E. G. Friedman, "Prediction of CMOS compatible on-chip optical interconnect," Integr. VLSI J. **40**(4), 434–446 (2007).
5. A. W. Fang, H. Park, O. Cohen, R. Jones, M. J. Paniccia, and J. E. Bowers, "Electrically pumped hybrid AlGaInAs-silicon evanescent laser," Opt. Express **14**(20), 9203–9210 (2006).
6. A. W. Fang, R. Jones, H. Park, O. Cohen, O. Raday, M. J. Paniccia, and J. E. Bowers, "Integrated AlGaInAs-silicon evanescent race track laser and photodetector," Opt. Express **15**(5), 2315–2322 (2007).
7. T. Tsuchizawa, K. Yamada, H. Fukuda, T. Watanabe, J. Takahashi, M. Takahashi, T. Shoji, E. Tamechika, S. Itabashi, and H. Morita, "Microphotonics devices based on silicon microfabrication technology," IEEE J. Sel. Top. Quantum Electron. **11**(1), 232–240 (2005).
8. R. Katouf, N. Yamamoto, A. Kanno, N. Sekine, K. Akahane, H. Sotobayashi, T. Isu, and M. Tsuchiya, "Ultrahigh relative refractive index contrast GaAs nanowire waveguides," Appl. Phys. Express **1**, 122101 (2008).
9. H. Enomoto, K. Inoue, T. Okumura, H. D. Nguyen, N. Nishiyama, Y. Atsumi, S. Kondo, and S. Arai, "Properties of high index-contrast wired GaInAsP waveguides with benzocyclobutene on Si substrate," The 21st IEEE International Conference on Indium Phosphide and Related Materials (IPRM2009), ThA1.4 (2009).
10. T. Okamoto, N. Nunoya, Y. Onodera, S. Tamura, and S. Arai, "Continuous wave operation of optically pumped membrane DFB laser," Electron. Lett. **37**(24), 1455–1457 (2001).
11. T. Okamoto, N. Nunoya, Y. Onodera, T. Yamazaki, S. Tamura, and S. Arai, "Optically pumped membrane BH-DFB lasers for low-threshold and single-mode operation," IEEE J. Sel. Top. Quantum Electron. **9**(5), 1361–1366 (2003).
12. T. Okamoto, T. Yamazaki, S. Sakamoto, S. Tamura, and S. Arai, "Low-threshold membrane BH-DFB laser arrays with precisely controlled wavelength over a wide range," IEEE Photon. Technol. Lett. **16**(5), 1242-1244 (2004).

#137725 - $15.00 USD Received 4 Nov 2010; revised 10 Dec 2010; accepted 5 Jan 2011; published 18 Jan 2011

13. S. Sakamoto, T. Okamoto, T. Yamazaki, S. Tamura, and S. Arai, "Multiple-wavelength membrane BH-DFB laser arrays," IEEE J. Sel. Top. Quantum Electron. **11**(5), 1174–1179 (2005).
14. S. Sakamoto, H. Naitoh, M. Ohtake, Y. Nishimoto, S. Tamura, T. Maruyama, N. Nishiyama, and S. Arai, "Strongly index-coupled membrane BH-DFB lasers with surface corrugation grating," IEEE J. Sel. Top. Quantum Electron. **13**(5), 1135–1141 (2007).
15. N. Nunoya, M. Nakamura, M. Morshed, S. Tamura, and S. Arai, "High-performance 1.55-μm wavelength GaInAsP-InP distributed-feedback lasers with wirelike active regions," IEEE J. Sel. Top. Quantum Electron. **7**(2), 249–258 (2001).
16. S. Sakamoto, H. Naitoh, M. Ohtake, Y. Nishimoto, T. Maruyama, N. Nishiyama, and S. Arai, "85 °C continuous-wave operation of GaInAsP/InP-membrane buried heterostructure distributed feedback lasers with polymer cladding layer," Jpn. J. Appl. Phys. **46**(47), L1155–L1157 (2007).
17. H. Naitoh, S. Sakamoto, M. Ohtake, T. Okumura, T. Maruyama, N. Nishiyama, and S. Arai, "GaInAsP/InP membrane BH-DFB laser with air-bridge structure," Jpn. J. Appl. Phys. **46**, 1158–1160 (2007).
18. T. Maruyama, T. Okumura, S. Sakamoto, K. Miura, Y. Nishimoto, and S. Arai, "GaInAsP/InP membrane BH-DFB lasers directly bonded on SOI substrate," Opt. Express **14**(18), 8184–8188 (2006).
19. T. Okumura, T. Maruyama, M. Kanemaru, S. Sakamoto, and S. Arai, "Single-mode operation of GaInAsP/InP-membrane distributed feedback lasers bonded on silicon-on-insulator substrate with rib-waveguide structure," Jpn. J. Appl. Phys. **46**(48), L1206–L1208 (2007).
20. K. Oe, Y. Noguchi, and C. Caneau, "GaInAsP lateral current injection lasers on semi-insulating substrates," IEEE Photon. Technol. Lett. **6**(4), 479–481 (1994).
21. E. H. Sargent, K. Oe, C. Caneau, and J. M. Xu, "OEIC-enabling LCI lasers with current guides: Combined theoretical-experimental investigation of internal operating mechanisms," IEEE J. Quantum Electron. **34**(7), 1280–1287 (1998).
22. T. Okumura, M. Kurokawa, M. Shirao, D. Kondo, H. Ito, N. Nishiyama, T. Maruyama, and S. Arai, "Lateral current injection GaInAsP/InP laser on semi-insulating substrate for membrane-based photonic circuits," Opt. Express **17**(15), 12564–12570 (2009).
23. T. Okumura, H. Ito, D. Kondo, N. Nishiyama, and S. Arai, "Continuous wave operation of thin film lateral current injection lasers grown on semi-insulating InP substrate," Jpn. J. Appl. Phys. **49**(4), 040205 (2010).
24. T. Okumura, M. Kurokawa, D. Kondo, H. Ito, N. Nishiyama, and S. Arai, "Lateral current injection type GaInAsP/InP DFB lasers on SI-InP substrate," The 21st IEEE International Conference on Indium Phosphide and Related Materials (IPRM2009), TuB2 (2009).
25. S. Sakai, M. Umeno, and Y. Amemiya, "Measurement of diffusion coefficient and surface recombination velocity for p-InGaAsP grown on InP," Jpn. J. Appl. Phys. **19**(1), 109–113 (1980).
26. J. Kang, K. Inoue, Y. Atsumi, N. Nishiyama, and S. Arai, "Loss measurement of multiple layer a-Si waveguides," International Conference on Solid State Devices and Materials (SSDM2010), D-8–2 (2010).
27. N. Nishiyama, C. Caneau, and C. E. Zah, "Long Wavelength VCSELs on InP grown by MOCVD," Proc. SPIE **5246**, 10–17 (2003).
28. T. Okumura, D. Kondo, H. Ito, S. Lee, D. Takahashi, N. Nishiyama, and S. Arai, "Dynamic characteristics of lateral current injection laser," The 37th International Symposium on Compound Semiconductors (ISCS 2010), WeE3–2 (2010).
29. K. Ohira, N. Nunoya, and S. Arai, "Stable single-mode operation of distributed feedback lasers with wirelike active regions," IEEE J. Sel. Top. Quantum Electron. **9**(5), 1166–1171 (2003).
30. T. Shindo, S. Lee, D. Takahashi, N. Tajima, N. Nishiyama, and S. Arai, "Low-threshold and high-efficiency operation of distributed reflector laser with wirelike active regions," IEEE Photon. Technol. Lett. **21**(19), 1414–1416 (2009).

1. Introduction

The scaling of silicon complementary metal oxide semiconductor (CMOS) technology has resulted in considerable advancements in large-scale-integration (LSI) circuits. However, it is predicted that the performance of LSI technology will soon hit a ceiling owing to global wiring data capacity with technological progress [1,2]. One promising approach to overcome this predicted problem is to replace the electrical global wiring on a chip with an optical interconnection [3–6]. Therefore, various research activities have been undertaken with special focus on optical wiring.

For a light source of optical interconnection, conventional semiconductor lasers used for long-haul optical fiber communication or optical recording are unsuitable in terms of their high power dissipation and large dimensions. Instead, photonic devices based on high-index-contrast waveguides have been attracting considerable attention for use in compact and low-power photonic integrated circuits (PICs) [7–9]. We previously proposed the use of a new type of distributed feedback (DFB) laser to enhance the optical confinement factor of an active layer by a factor of about 3; this enhancement was aimed at reducing the threshold

#137725 - $15.00 USD Received 4 Nov 2010; revised 10 Dec 2010; accepted 5 Jan 2011; published 18 Jan 2011

current without compromising on the external quantum efficiency. The laser consists of a semiconductor membrane structure, in which the thin active waveguide (approximately 150 nm) is sandwiched between low-refractive-index benzocyclobutene (BCB) or SiO_2 cladding layers. Then, we demonstrated a room-temperature continuous-wave (RT-CW) operation of the proposed laser under optical pumping [10–13]. Thus far, a threshold pump power as low as 0.34 mW with a stable single-mode operation of the membrane DFB laser has been achieved under an RT-CW condition [14] by adopting wire-like active regions with surface corrugation to realize a strong index-coupling structure [15]. Further, a CW operation temperature of up to 85°C has been attained without special heat-sinking geometry [16]. In addition, a membrane DFB laser with an air bridge structure [17] and a membrane DFB laser bonded on a silicon-on-insulator (SOI) substrate for silicon PICs [18,19] were fabricated under optical pumping and the RT-CW condition. With the aim of realizing injection-type membrane lasers, we introduced a lateral-current-injection (LCI) structure [20,21]; i.e., we fabricated LCI- Fabry-Pérot (FP) [22,23] and LCI-DFB [24] lasers consisting of compressively strained multiple quantum wells (CS-MQWs) with a 400-nm-thick GaInAsP core layer grown on a semi-insulating (SI) InP substrate.

In this study, we fabricated a novel LCI-DFB laser having an amorphous Si (a-Si) surface grating structure. The fabrication involved three-step epitaxial growth and subsequent electron-beam lithography (EBL) of the a-Si surface grating.

2. Device structure and fabrication

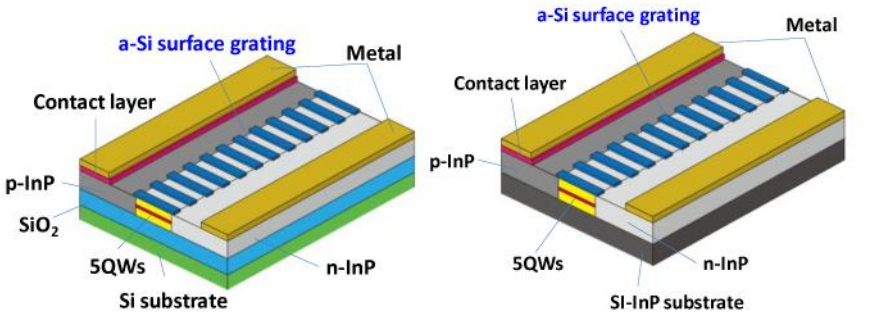

(a) Membrane DFB laser on Si substrate (b) LCI-DFB laser on SI-InP substrate

Fig. 1. Schematic structures of LCI-DFB lasers with a-Si surface grating on Si and SI-InP substrates.

Our final target is a current-injection-type membrane DFB laser bonded on a Si substrate by SiO_2, as shown in Fig. 1(a), wherein a buried heterostructure is formed along the lateral direction with n-InP and p-InP cladding layers. Air and SiO_2 are the upper and lower claddings, respectively. The a-Si surface grating is formed on the stripes. However, in this study, to simplify the fabrication process for verifying the effect of the a-Si surface grating on the performance of the LCI laser, we fabricated the LCI-DFB laser on an SI-InP substrate without bonding the laser to the Si substrate, as shown in Fig. 1(b), and investigated its fundamental operation characteristics.

Figure 2 shows the fabrication process of the LCI-DFB laser with the a-Si surface grating. An initial wafer with an undoped GaInAsP core layer was grown on an Fe-doped SI-InP substrate by organometallic vapor phase epitaxy (OMVPE); the core layer included the lower optical-confinement layer (OCL, λ_g = 1.2 μm, 140-nm thick), five 1% compressively strained

#137725 - $15.00 USD Received 4 Nov 2010; revised 10 Dec 2010; accepted 5 Jan 2011; published 18 Jan 2011

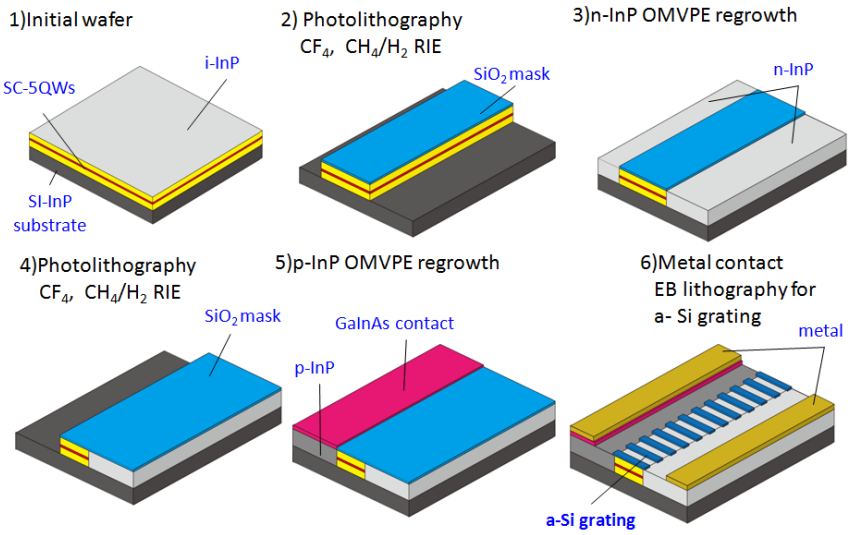

Fig. 2. Fabrication process of LCI-DFB laser with a-Si surface grating

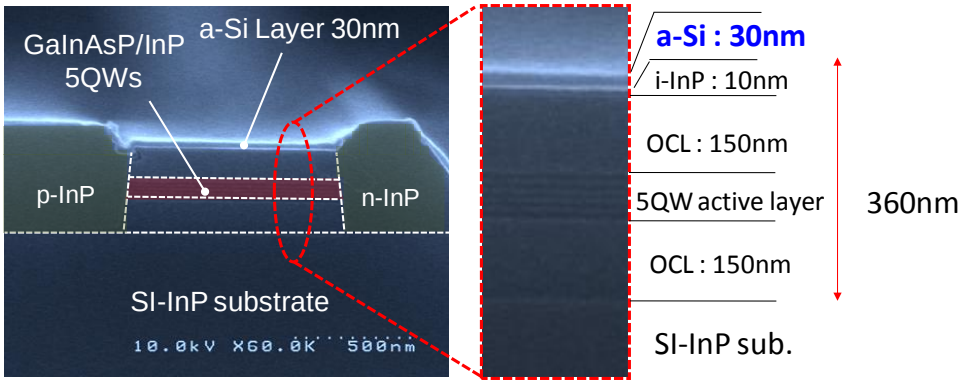

Fig. 3. Cross-sectional SEM image of fabricated LCI-DFB laser with a-Si surface grating

$Ga_{0.22}In_{0.78}As_{0.81}P_{0.19}$ QWs (6-nm-thick well), 0.15% tensile-strained barriers (10 nm), an upper OCL (λ_g = 1.2 μm, 140-nm thick), and an undoped thin (10 nm) InP layer. This thin InP layer was introduced to prevent exposure of the upper GaInAsP OCL which has high surface recombination speed [25]. The total thickness of the GaInAsP core layer was 360 nm; as a result, the optical confinement factor of the active layer would be almost equal to that of a conventional double heterostructure with a thick cladding layer. Then, the LCI structure was fabricated by CH_4/H_2 reactive ion etching (RIE) and two-step OMVPE selective-area growth. First, 7-μm-wide and 360-nm-high mesa structures were fabricated with a SiO_2 mask. After the removal of damaged surfaces on both sides of the mesa structures resulting from dry etching by wet chemical cleaning, n-InP ($N_d = 4 \times 10^{18}/cm^3$) was selectively regrown on both sides of the mesa structures as a cladding layer. Next, narrow (2-μm wide) stripes were formed so as to enable fundamental transverse mode operation. After etching the part of the mesa and the other side of the n-type cladding layer, p-InP ($N_d = 4 \times 10^{18}/cm^3$) and p-GaInAs ($N_d = 8 \times 10^{18}/cm^3$) were regrown on a side of the mesa structure in the same way. Then, the part of the GaInAs contact layer near the stripe edge was removed by wet chemical etching to reduce optical absorption. Next, Ti/Au electrodes were evaporated onto the p-contact and the n-InP areas and a contact pads were formed by lift-off process.

#137725 - $15.00 USD Received 4 Nov 2010; revised 10 Dec 2010; accepted 5 Jan 2011; published 18 Jan 2011

Then, the a-Si surface grating structure was fabricated. After a 30-nm thick a-Si layer was deposited on the wafer by plasma-enhanced chemical vapor deposition (PECVD), 10-μm-wide surface grating patterns were formed by EBL and subsequent CF_4 inductively coupled plasma etching. It is noteworthy that we had previously confirmed negligible absorption of our a-Si film by fabricating low-loss a-Si wire waveguides [26]. Here, the depth of the a-Si surface grating was set to 30 nm, because a very deep (200 nm) surface grating structure would result in cutting-off of the fundamental transverse mode in the vertical direction. The index-coupling coefficient κ_i was estimated to be 100 cm^{-1} for the grating depth of 30 nm. Finally, the unwanted a-Si layer on the electrode pads was removed by CF_4 RIE. The laser cavity was formed by cleaving without any facet coating. Figure 3 shows the cross-sectional scanning electron microscopy (SEM) image of the fabricated LCI-DFB laser with a-Si surface grating. Even though both sides of the mesa stripes became slightly thicker (around 100 nm) than the center of the mesa structure owing to selective-area growth with a relatively wide (7 μm) SiO_2 stripe mask, the optical mode field confinement can be defined by the refractive-index difference between the MQWs with OCLs and the InP cladding layers.

3. Device characteristics

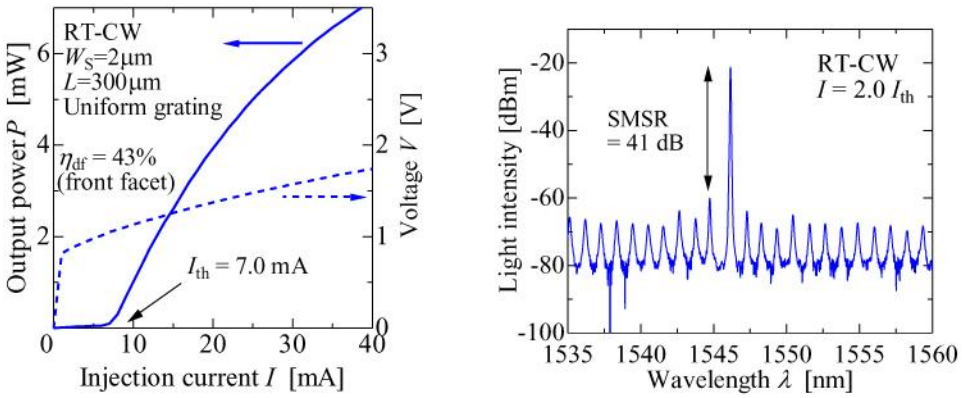

Fig. 4. (a) I-L and I-V curves and (b) lasing spectrum of LCI-DFB laser with a-Si surface grating

Figure 4(a) shows current-light output (*I-L*) (solid line) and voltage-current (*V-I*) characteristics (dashed line) of the LCI-DFB laser with a-Si surface grating under the RT-CW condition. The cavity length and stripe width were 300 μm and 2.0 μm, respectively. The grating coupling strength $\kappa_i L$ was estimated to be around 3.0. A threshold current (I_{th}) of 7.0 mA and a differential quantum efficiency from the front facet (η_{df}) of 43% were obtained. This threshold current is the lowest and the differential quantum efficiency from a single facet is the highest among all LCI-type lasers reported thus far. The differential series resistance and the voltage at the threshold current were around 25 Ω and 1.1 V, respectively. For realization a current injection type membrane laser, the thermal problems due to large series resistance is expected to be an important issue. To solve this issue without sacrificing the advantage of low threshold current operation of the membrane lasers, we have to reduce both electrical resistance and thermal resistance. In the fabricated device, the interval between the stripe and the electrode in p-doped InP region was 3 μm, and the p-doped InP layer thickness was about 360 nm. Given a high sheet resistance of 2.7 kΩ/□ in this area [23], the resistance in p-doped InP region occupied the large part of the series resistance. Therefore, reducing the interval between the stripe and the electrode may be inevitable for membrane lasers.

About thermal resistance, in previously reported LCI-FP laser which has similar structure to the current device, we estimated the thermal resistance of about 200 K/W [23]. The LCI laser based on the membrane structure is expected to have higher thermal resistance

#137725 - $15.00 USD Received 4 Nov 2010; revised 10 Dec 2010; accepted 5 Jan 2011; published 18 Jan 2011

compared with the LCI laser on SI-InP substrate. However, we expect that the thermal resistance of the LCI-membrane laser can be the same level of the long wavelength vertical cavity surface emitting laser [27] by optimizing heat radiation from metal electrodes and so on. In addition, an expected driving current of the membrane laser is a few orders of magnitude smaller than that of conventional laser for on-chip interconnection [3], the heat generation from the membrane laser itself by injected current is expected to be negligible. Actually a continuous wave operation of membrane DFB laser was realized up to 85°C under optical pumping even though it had poor heat-sinking structure (only 150 nm thick semiconductor membrane structure sandwiched between BCB polymer) than the fabricated device [16]. Thus, the membrane LCI-DFB laser can operate at higher temperatures by adopting an appropriate design of metal contacts.

Figure 4(b) shows the lasing spectrum of the proposed laser. As can be seen from the figure, a lasing wavelength of 1546 nm and a side-mode suppression ratio (SMSR) of 41 dB were obtained at a bias current twice the threshold current (I = 14.0 mA). Since the index-coupling coefficient κ_i was not higher than that of previously reported DFB lasers with wire-like active regions, a clear stopband was not observed, but a resonant mode spacing of about 1 nm was observed, which corresponds to FP resonance at a cavity length of 300 μm.

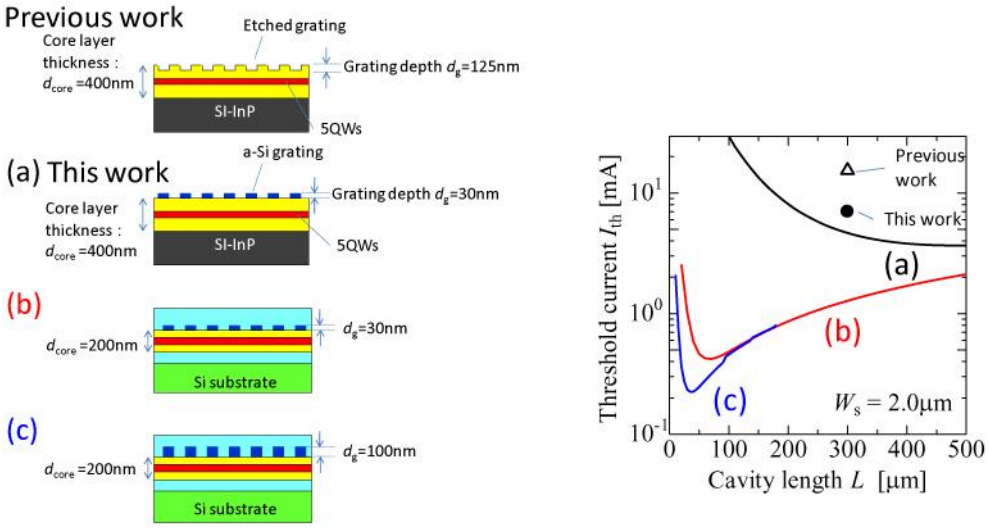

Fig. 5. Cavity length dependence of threshold current of various LCI-DFB lasers with a-Si surface grating.

Next, the theoretical threshold current of the proposed 5-QW LCI-DFB laser with a-Si surface grating on the SI-InP substrate was calculated and compared with that obtained experimentally. Figures 5(a)–(c) show the dependence of threshold current of three types of LCI-DFB lasers with a-Si surface grating on cavity length—a laser with a structure similar to that of the fabricated laser (core thickness 400 nm, SI-InP substrate, a-Si surface grating depth of 30 nm), a membrane LCI-DFB laser with an a-Si surface grating depth of 30 nm, and a membrane LCI-DFB laser with a deep surface grating of 100 nm, respectively. In this theoretical calculation, the strip width was assumed to be 2 μm and the carrier concentration profiles of electrons and holes were assumed to be uniform along the stripe width direction. For comparison, the normalized threshold current of our previous LCI-DFB laser with 125 nm directly etched surface grating structure [24] is also plotted in Fig. 5 (triangle). In this result, the threshold current of 27 mA was obtained for the laser stripe width of 3.5 μm, and cavity length of 300 μm. Please note the point of the previous results in Fig. 5 is normalized by 2.0-μm stripe width (the corresponding threshold current is 15.4 mA) for fair comparison. Meanwhile, the threshold current (I_{th} = 7.0 mA) of the fabricated LCI-DFB laser with a-Si

#137725 - $15.00 USD Received 4 Nov 2010; revised 10 Dec 2010; accepted 5 Jan 2011; published 18 Jan 2011

surface grating (circle in Fig. 5) was reduced by half compared with the previous device although the grating depth was deeper for the previous result. We believe this is because the direct semiconductor etching to such thin semiconductor layer may cause optical and electrical losses by several effects. As a calculated result, the theoretical threshold current of the LCI-DFB laser with a-Si surface grating on the SI-InP substrate was found to be 4.7 mA for the cavity length of 300 μm, which is about 30% lower than the experimentally obtained value. Since the index-coupling coefficient (100 cm^{-1}) is fairly low, the lowest threshold current of 3.7 mA occurred at a cavity length of 450 μm.

The experimentally obtained threshold current value of 7 mA might be attributed to the slightly low grating coupling coefficient. If the InP substrate is replaced with a SiO_2/Si substrate, the threshold current of the membrane LCI-DFB lasers will become around 1.2 mA at the cavity length of 300 μm, and it will be much lower threshold current of about 0.2 mA with much shorter cavity lengths due to enhanced optical confinement factor into the active region as well as the higher grating coupling coefficient.

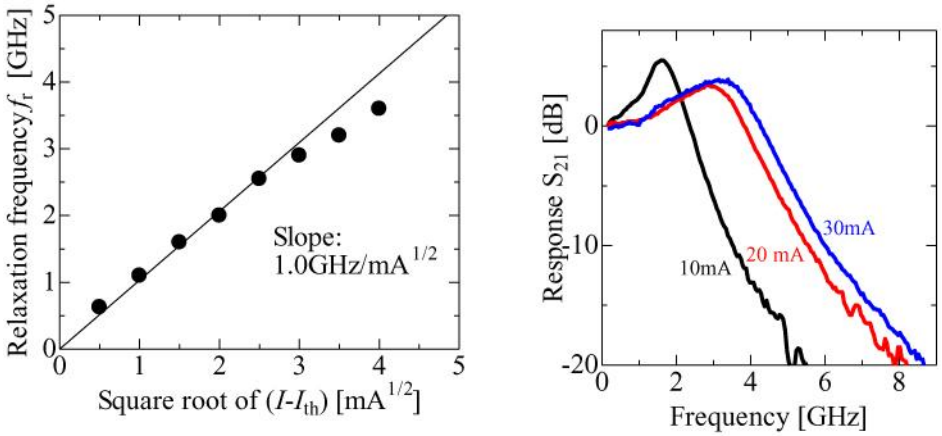

Fig. 6. Direct modulation characteristics of LCI-DFB laser; (a) relaxation oscillation frequency as a function of square root of bias current and (b) small-signal modulation response.

Next, direct modulation characteristics of the proposed LCI-DFB laser were measured after bonding it on an AlN coplanar sub-mount for high-speed measurements. Figure 6(a) shows the dependence of the relaxation oscillation frequency (f_r) on the square root of bias current above the threshold $(I - I_{th})^{1/2}$. Here, f_r was measured as the peak frequency of relative-intensity-noise (RIN) spectrum. The modulation current efficiency factor (MCEF) of the laser was approximately 1.0 GHz/$mA^{1/2}$, which is at least twice that of the previously reported LCI-FP lasers [28]. As can be seen in the I-L property in Fig. 4, the light output saturated when the injected current was over about 15 mA due to heating. Therefore, the saturation of MCEF was also attributed to the gain saturation due to the thermal effect. The value can be improved by increasing the internal quantum efficiency by adopting higher bandgap material as barrier layers and both sides of OCLs. Figure 6(b) shows the small-signal modulation response (S_{21}) of the laser as measured by a network analyzer. For this measurement, the bias current applied to the laser was varied from 10 to 30 mA. A small-signal modulation bandwidth of 4.8 GHz was obtained at a bias current of 30 mA. This bandwidth may be attributed to the higher internal quantum efficiency and shorter cavity length than those of previously reported LCI-FP lasers [28].

The RC product of the LCI type laser is expected to be relatively low compared with the conventional vertical junction laser structure due to the low parasitic capacitance in the LCI structure [20]. Thus, the limitation of the modulation bandwidth was attributed to the saturation of the MCEF.

#137725 - $15.00 USD Received 4 Nov 2010; revised 10 Dec 2010; accepted 5 Jan 2011; published 18 Jan 2011

In our final target of the light source for the on-chip interconnection, the requirement of the modulation speed of the device is assumed to be 10 Gb/s in each channel. For this purpose, a much higher MCEF and following higher modulation bandwidth are needed and it can be expected to be obtained by improving the internal quantum efficiency and introducing higher-index-coupling grating structure such as wire-like active regions into the proposed laser [29,30].

4. Conclusion

In conclusion, a lateral current injection (LCI)-type DFB laser with a-Si surface grating was fabricated on an SI-InP substrate and its successful operation under an RT-CW condition was demonstrated. A threshold current 7.0 mA and an external differential quantum efficiency from the front facet of 43% were obtained for a device with a stripe width of 2.0 μm and cavity length of 300 μm. We expect that application of this LCI structure to a membrane structure with a high-index-contrast waveguide will yield lasers with much lower power consumption having potential for use in on-chip optical interconnects.

Acknowledgments

We would like to thank Professors Emeritus Y. Suematsu and K. Iga for their continuous encouragement and Professors M. Asada, F. Koyama, T. Mizumoto, Y. Miyamoto, and Dr. SeungHun Lee of the Tokyo Institute of Technology for fruitful discussions. This research was financially supported by Grants-in-Aid for Scientific Research (#19002009, #22360138, #21226010, #08J55211, and #10J08973) from the Ministry of Education, Culture, Sports, Science and Technology (MEXT), Japan, and the Japan Society for the Promotion of Science (JSPS)-FIRST Program. The first author would like to acknowledge the JSPS for the Research Fellowship for Young Scientists.

#137725 - $15.00 USD Received 4 Nov 2010; revised 10 Dec 2010; accepted 5 Jan 2011; published 18 Jan 2011